STU SvF
SLOVAK UNIVERSITY OF TECHNOLOGY IN BRATISLAVA
FACULTY OF CIVIL ENGINEERING

Slovak Journal of Civil Engineering

Vol. 33, 2025, No. 4, 54– 66
DOI: 10.2478/sjce-2025-0027

INVESTIGATING THE CHANGES IN THE GROUNDWATER FLOW REGIME DURING THE MOST RECENT HIGH FLOODS IN BUDAPEST

Flóra WAGNER[1*]

Abstract

Groundwater and surface water have a strong relationship in riverside municipal areas, although obstructed by buildings with underground structures that reach the aquifer. In the study area of Lágymányos (Budapest, Hungary), the groundwater level is highly influenced by the Danube. This research investigates these exchange processes in the case of a flood, and their changes resulting from the construction of two riverside buildings. These buildings were built between the earlier floods in 2010 and 2013 and the recent floods in 2023 and 2024. The specific groundwater discharge was computed by frequently monitoring the groundwater levels. The results are compared to the water level of the Danube and result in loop rating curves. These are approached with ellipses to examine their estimation. If obstructed, the parameters of the ellipses change for the earlier and newer floods. The calculations were also investigated at wells with no underground structures nearby. Further investigations could lead to an easier quantifying of the specific groundwater discharge.

Address

[1] Dept. of Hydraulic and Water Resources Engineering, Budapest University of Technology and Economics, Budapest, Hungary

[*] ***Corresponding author:*** wagner.flo a@emk.bme.hu

Key words

- Groundwater fl w,
- Municipal area,
- Underground structures,
- The Danube River,
- Interaction of groundwater and surface water,
- Floods.

1 INTRODUCTION

Quantifying exchange processes between groundwater and surface water is an important topic from both perspectives. During flood waves, it is essential to know the amount of the discharge exiting from a river and any changes due to the obstruction of the riverside with underground structures that reach the aquifer. The measurement of the groundwater flow is also a complicated process (Kalbus et al., 2006), as it is not directly visible, and any changes in the flow through interaction with the surface water do not appear immediately. Any change in the groundwater flow is also important from the aspect of the structures in the urban areas (Godlewski et al., 2019), as long-term low water table periods can cause reactivated consolidation processes in soils that are prone to it. In addition to the expected peak river water level and durability, the groundwater level also has a significant role when planning flood protection measures. It may be worth assessing the groundwater level conditions of any protected areas and thus making the protection against flood phenomena influenced by groundwater level distributions more effective, because in 2013, more flood failures developed due to the higher initial groundwater level detected in the area (Nagy, 2025).

In this study, an estimation of specific discharges, using data series before and after two large riverside constructions, is examined. This could help during the modelling of flood events and bank storage and provide a deeper understanding of the characteristics of the groundwater - surface water interaction. The changes in this relationship can only be discovered if data series presenting measurements of water tables over a longer period are available.

2 METHOD

A good example of the change in the groundwater flow in an urban area is the Lágymányos study area called INFOPARK in Budapest, Hungary, where the groundwater level is highly affected by the river Danube; the area is constantly expanding with the construction of new university and office buildings. This makes the Lágymányos study area a highly investigated area with plenty of data and possibilities.

The groundwater level monitoring has been going on for more than 20 years up to this day. The flood of 2010 and the record-breaking flood of 2013 were followed by 10 years of low water levels, including the lowest water level ever recorded. Two new riverside office buildings with underground garages were built in this time period. The next high floods occurred in December of 2023 and in June and September of 2024. This afforded an opportunity to examine the newly obstructed groundwater flow with two sets of data series before and three after the construction works.

2.1 Background of the computations

During low water levels in a river, the groundwater flows towards the river, which is then called the gaining stream (Fig.1, right). During floods, this relation reverses, and the river loses water (Fig.1, left); it infiltrates into the surrounding groundwater, and the level of the groundwater rises. In this study this water loss during flood events is also estimated. The groundwater specific discharge is calculated with Darcy's equation, which is a fundamental equation of the flow of fluid through porous media such as groundwater.

The slope in one section is determined by Eq. 1 for sections perpendicular to a river and Eq. 2. for sections parallel to a river, and is noted with S [-]. The water level at the end points of the sections is h [m a.s.l.], and r [m] is the distance between them. This means that the groundwater's specific discharge would be negative, when the groundwater flows from the direction of the river along the section, so the river loses water (Fig. 1, left); when the groundwater flows into the river, it would be positive, and the river would gain water (Fig. 1, right).

The Darcy velocity of the groundwater flow is determined by Eq. 3, where v is the Darcy velocity in the section [m/s]; S is the above-defined slope of the section [-]; and k is the hydraulic conductivity [m/s] in the section. If this is the velocity component perpendicular to the river, that is of major importance from the point of view of the river-groundwater connection.

$$S_{perpendicular} = (h_{Well} - h_{Danube\ or\ riverside\ well})/r \quad (1)$$

$$S_{parallel} = (h_{Southern\ well} - h_{Northern\ well})/r \quad (2)$$

$$v = S \cdot k \quad (3)$$

The specific groundwater discharge is noted with q [m2/s] and is determined by Eq. 4, where H [m] is the difference between the groundwater level and the level of the base, which is the saturated thickness of the aquifer.

$$q = v \cdot H \quad (4)$$

3 DESCRIPTION OF THE CONDITIONS OF THE STUDY AREA

3.1 Geological data

The Lágymányos part of the Danube previously had a wide, degraded bed with sand banks, especially on its right side. After a catastrophic ice flood in 1838, a parallel structure was built to narrow and deepen the river. Behind the parallel structure, the former river bed was gradually filled from the north to the south. Several large-scale constructions have taken place; one of the newest sites is the INFOPARK, which contains university and office buildings (Fig. 2).

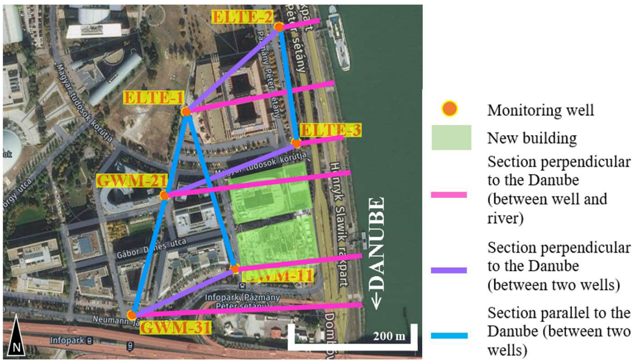

Fig. 2 *The INFOPARK study area in Lágymányos, Budapest, with the six monitoring wells and the two newest buildings; the sections examined are portrayed with lines*

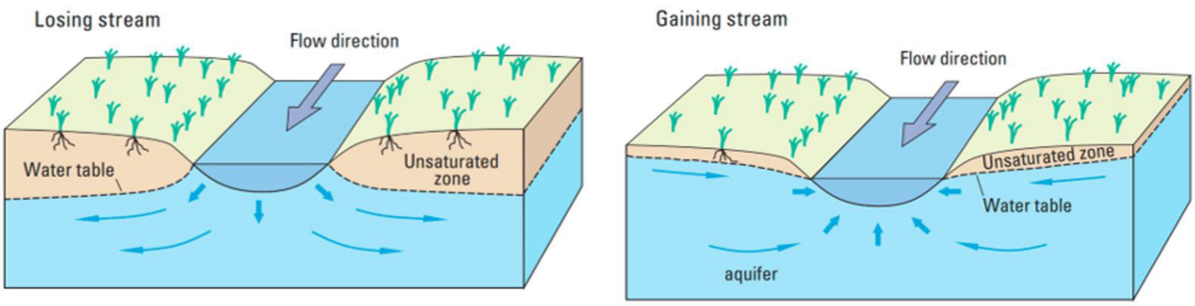

Fig. 1 *Scheme of the process of the interaction of the surface flows with the groundwater (Winter et al., 1998)*

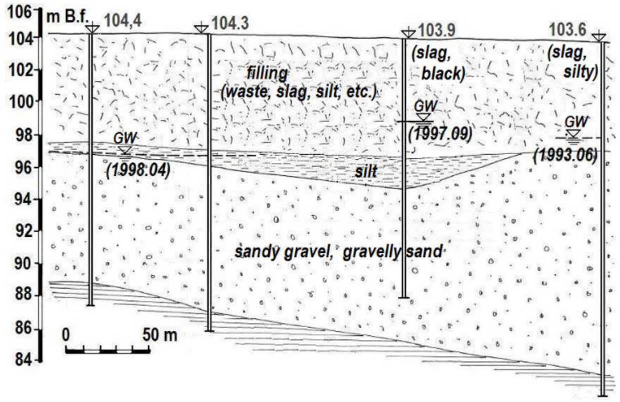

Fig. 3 *A typical section of the aquifer (Csoma and Gálos, 2012)*

The filling of the area is a mixed material, with the main component being slag from a nearby power station (Csoma and Gálos, 2012). The area has different layers. The top layer is a mixed filling with a thickness of 6 – 8 m (hydraulic conductivity: $1.5{\cdot}10^{-5}$ m/s – $3{\cdot}10^{-5}$ m/s). A thin (1-2 m) layer of silt (hydraulic conductivity: $7{\cdot}10^{-10}$ m/s – $7{\cdot}10^{-8}$ m/s) is present in some places. These show less permeable soil than the next layer, i.e., the aquifer, which is a partly gravel and partly sandy gravel layer of river sediment. It is 10 - 12 m thick and has a relatively high hydraulic conductivity ($2.9{\cdot}10^{-3}$ m/s – $1.3{\cdot}10^{-2}$ m/s). The base of the aquifer is partly clay and partly clayey marl below the bottom of the river. A typical section of the aquifer is shown in Fig. 3. The hydraulic conductivity used along the sections is estimated according to the values found in Szívós et al., 2013. The level of the base is between 90 and 92 m a.s.l.; it was estimated according to previous research (Wagner, 2018) and maps (Horusitzky, 1932).

3.2 Changes in the conditions of the study area

Since the 2000s, a number of modern university and office buildings have been built in INFOPARK, which is one of the newest areas in Budapest. Most of them have multi-storey underground garages, with structures reaching the aquifer. They have an impact on the groundwater and affect the direction of the flow. Because of these interventions, the long data series of the area is inhomogeneous; its processing is discussed in a previous work (Wagner, 2022).

After floods in 2010 and 2013, two new buildings were built (see Fig. 2 in green). The construction of the Ericsson headquarters was finished in 2018. It has a four-storey underground garage; at its deepest point it is 21 meters below the ground. Its foundation level is estimated at 83.70 m a.s.l. The newest building is the Evosoft headquarters, which is located south of the Ericsson headquarters. It was completed in 2021. It also has a four-storey underground garage, and its foundation level is set at 83.70 m a.s.l.

3.3 Monitoring

As shown according to their names on Fig. 2, the Lágymányos study area has six working monitoring wells. The two direct riverside wells are the ELTE-2 and ELTE-3, while the ELTE-1, GWM-11 and GWM-31 wells are located behind the buildings. The GWM-21 well has the most buildings around it.

The value of the groundwater level is manually monitored once a month with a groundwater meter that turns the light of a bulb on when the water level is reached. During high floods, the author manually monitors the water levels of the six wells more frequently, i.e., mostly daily, to ensure the recording of the data. Groundwater levels for the two earlier floods in 2010 and 2013 were available from previous work (Kukucska et al., 2015). The data used for the floods in 2023 and 2024 in this study are the author's own manual measurements.

The water level of the river Danube is available at the website of the General Directorate of Water Management (https://data.vizugy.hu/). The water level of the Danube applied at 1643.5 rkm is the daily average water level interpolated between the gauges at Vigadó Square (1646.5 rkm) and Kvassay-barrage (1642.2 rkm).

4 DATA SERIES OF THE WATER LEVELS

Figs. 5 – 10 show the manually measured groundwater level of the wells and the water level of the Danube (Fig. 4). These time series are adjusted so that the origin of the coordinate system is located at the time of the peak of each flood under study. That is how different floods can be compared, and also how the time delay between the highest water level of the Danube and each well can be tracked. In riverside wells (ELTE-2, ELTE-3) this time delay is one day, while the groundwater level during the flood in the GWM-21 well peaks up to five days later.

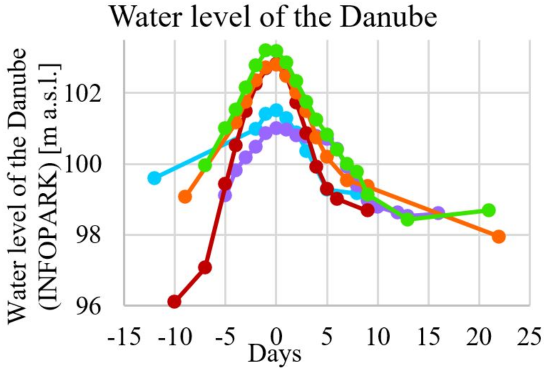

Fig. 4 *Data series of the water level of the Danube for the five floods examined*

Legend for Figs. 4-10.:
- Flood in June, 2010
- Flood in June, 2013
- Flood in December, 2023
- Flood in June, 2024
- Flood in September, 2024

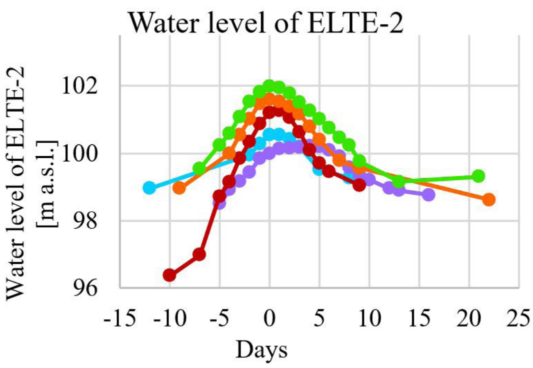

Fig. 5 *Groundwater level of ELTE-2 for the five floods examined*

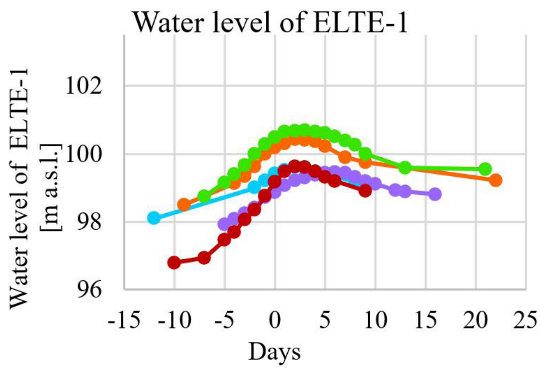

Fig. 6 *Groundwater level of ELTE-1 for the five floods examined*

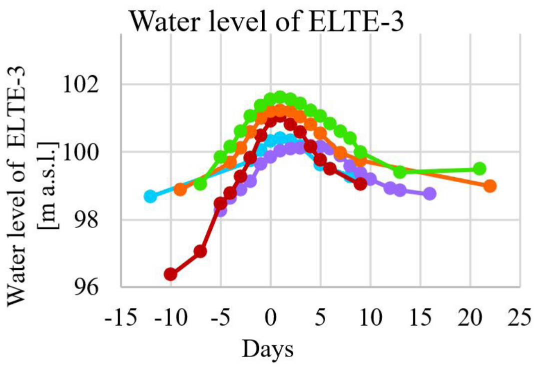

Fig. 7 *Groundwater level of ELTE-3 for the five floods examined*

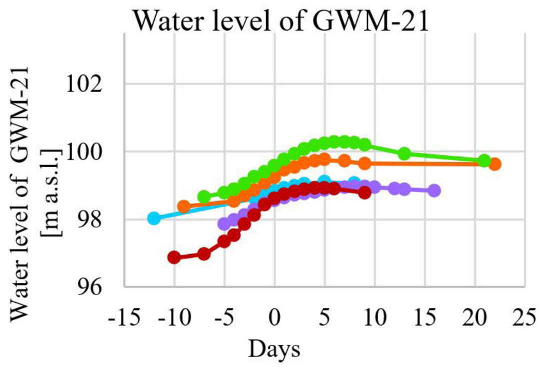

Fig. 8 *Groundwater level of GWM-21 for the five floods examined*

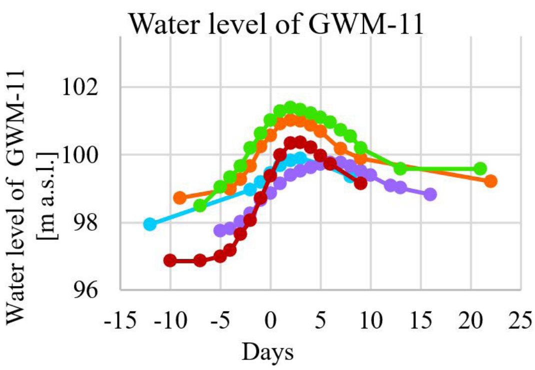

Fig. 9 *Groundwater level of GWM-11 for the five floods examined*

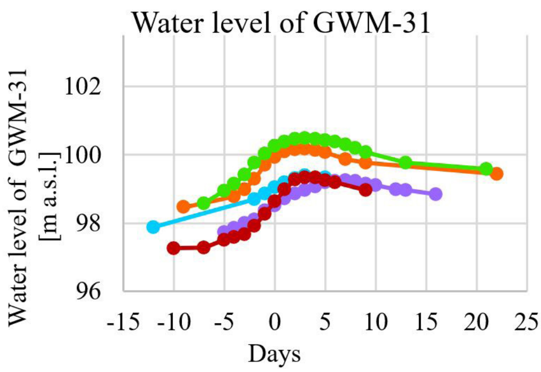

Fig. 10 *Groundwater level of GWM-31 for the five floods examined*

It can be seen that the highest water level of the last flood on the Danube approaches the 2010 and 2013 levels; while this also shows up in the riverside wells, this is not the case for the more distant wells. The peak groundwater levels are mainly not approaching the previous higher levels, especially behind the new buildings. Our next goal was to quantify this change.

As each flood is unique, a raw comparison of the groundwater level does not provide sufficient information about the changes. However, examining the changes in other additional quantities can be more characteristic of different situations. Thus, the specific discharge of groundwater is chosen as another indicator, and it is computed in several sections.

5 DISCUSSION OF THE RESULTS

Using Darcy's equation (Eq. 1 or Eq. 2, based on the direction), it is possible to examine several sections, which are shown in Fig. 2. Six of them are between the wells and the Danube, and they are perpendicular to the river, as shown with the pink lines. The three purple sections are between the wells and are perpendicular to the river to some degree. The four blue sections are also between wells, but they are roughly parallel to the Danube.

The calculation process is presented between ELTE-2 and the Danube for the five floods. When comparing the groundwater level with the water level of the Danube, loop curves can already be observed (shown in Fig. 11). Fig. 11 shows that the flood in September approached the peak level of 2010, but the groundwater level in the wells did not approach the maximum of 2010. Then, the slopes for the sections were calculated by Eq. 1 in that case and presented in Fig. 12. Eq. 3 was used for the Darcy velocity, which can be seen in Fig. 13. Fig. 14 shows the specific groundwater discharge, which was calculated with Eq. 4.

In the case of the riverside ELTE-2, a greater slope occurred in September of 2024 than in the higher flood of 2013. At the start of the flood, the level of the groundwater was lower, which means that during September of 2024, the background flow was smaller than in 2013. This condition meant a greater difference in the water level between the well and the river, which resulted in a greater velocity and specific discharge for the seepage from the river. This may refer back to the droughts in 2022 and 2024.

If the specific groundwater discharges are on the x-axis and the water level of the Danube is on the y-axis, then comparable loop curves will be formed in each section, similarly to the river hysteresis curve. The aim of this study was to further analyze the visible differences between these hysteresis curves in a simple way and describe them. The form of the curve indicated that it is approachable with an elliptical equation, the mathematical description of which is easier and which makes the calculations more understandable. The least squares method was used (Hendel, 2008) for the approximation; the data with a lower water level was not used for the earlier flood on sections GWM-21 – ELTE-3 and GWM-21 – ELTE-1, as the loop curve had several crossings. This process results in the following elliptical parameters: the rotation angle, semi-major and semi-minor axes, and the coordinates of the centre of the ellipses. Tab. 1 presents the ranges of the semi-major and semi-minor axes, and the rotation angle.

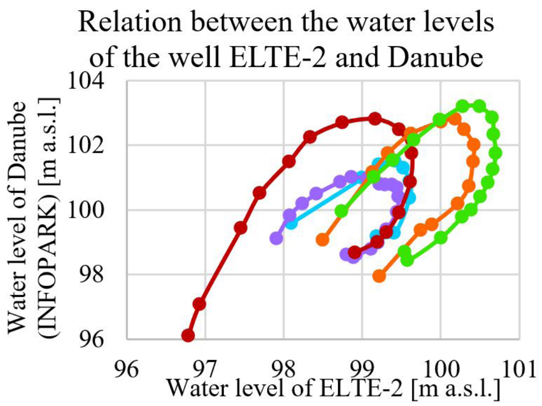

Fig. 11 *Groundwater level of ELTE-2 presented with the water level of the Danube*

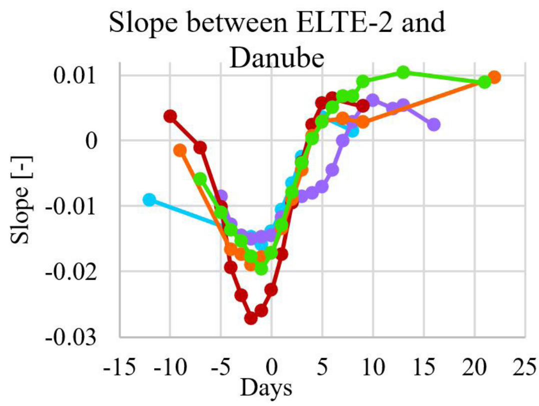

Fig. 12 *Slope in the section between the Danube and ELTE-2 (The negative value means losing the stream)*

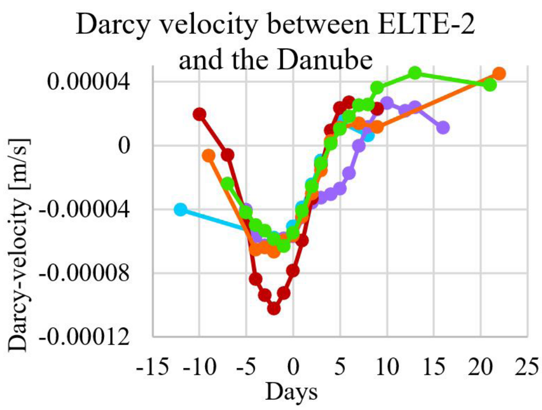

Fig. 13 *Calculated Darcy velocity on the section between the Danube and ELTE-2*

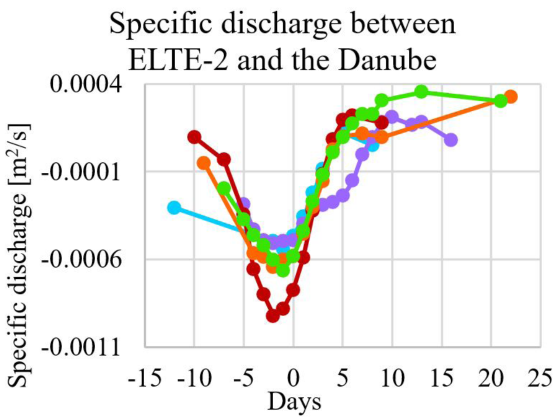

Fig. 14 *Specific discharge calculated on the section between Danube and ELTE-2*

Legend for Figs. 11-14.:

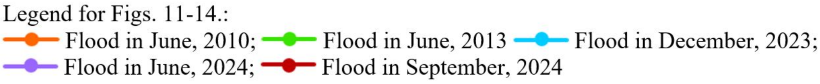

Tab. 1 *Range of values for the semi-major axis, semi-minor axis, and the rotation angle*

		Elte-2 - Danube	Elte-1 - Danube	Elte-3 - Danube	Gwm-21 - Danube	Gwm-11 - Danube	Gwm-31 - Danube	Elte-1 - Elte-2	Gwm-21 - Elte-3	Gwm-31 - Gwm-11	Elte-1 - Gwm-21	Gwm-21 - Gwm-31	Elte-1 - Gwm-11	Elte-2 - Elte-3	Value range	
Semi-major axis [m]	2010														Min: 1.12499	Max: 6.66405
	2013															
	2023.12.															
	2024.06.															
	2024.09.															
Semi-minor axis [m²/s]	2010														Min: $3{,}3067 \cdot 10^{-6}$	Max: $4{,}0082 \cdot 10^{-4}$
	2013															
	2023.12.															
	2024.06.															
	2024.09.															
Rotation angle [rad]	2010														Min: 1.57078	Max: 1.57107
	2013															
	2023.12.															
	2024.06.															
	2024.09.															

The rising limb of the flood is typically the lower part of an ellipse; the falling limb is the upper part. The nature of the loop curves is different if the sections are perpendicular or parallel to the Danube. The data calculated is presented with points, the ellipses are presented with dashed lines on the figures. These ellipses provide an approximate description of the system's behavior. For an accurate risk assessment and an engineering design, it would be more appropriate to preserve the actual hysteresis shape.

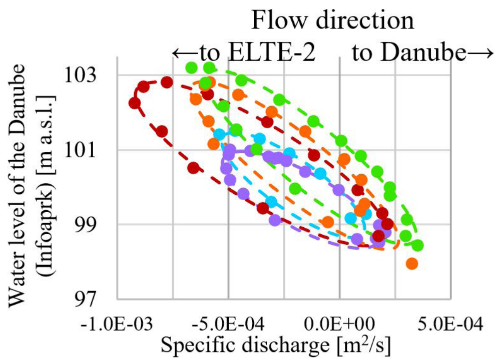

Fig. 15/ a *ELTE-2 and Danube*

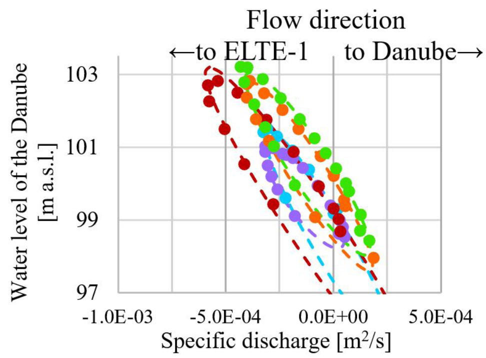

Fig. 15/ b *ELTE-1 and Danube*

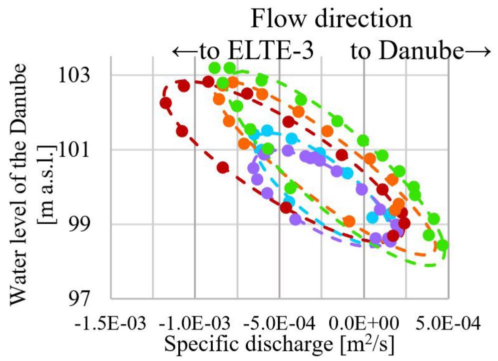

Fig. 15/c *ELTE-3 and Danube*

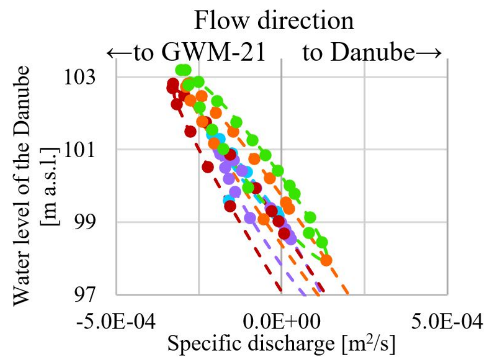

Fig. 15/d *GWM-21 and Danube*

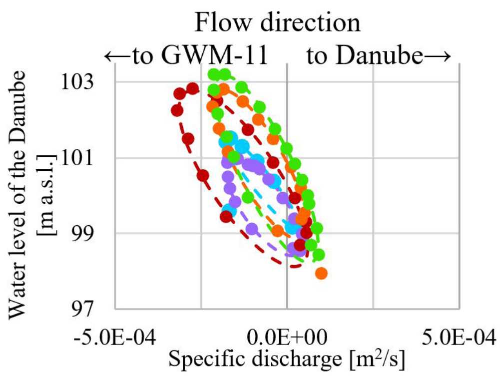

Fig. 15/e *GWM-11 and Danube*

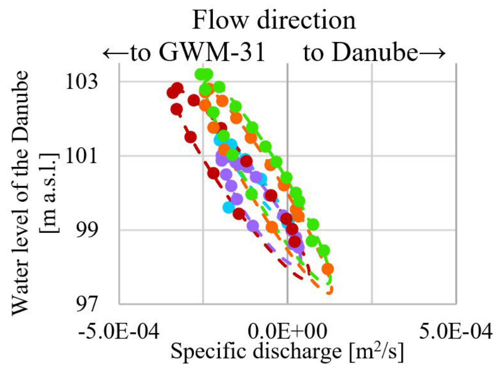

Fig. 15/f *GWM-31 and Danube*

Fig. 15 *Specific discharges in the sections between a well and the Danube (Infopark)*

Legend for Fig. 15:
Flood in June, 2010; Flood in June, 2013; Flood in December, 2023
Flood in June, 2024; Flood in September, 2024

Fig. 15 presents the sections between the wells and the Danube (shown in pink in Fig. 2). A shift between the earlier floods and the newer floods, which caused a greater discharge in September 2024, is visible. At the same water level of the Danube, greater discharge values have occurred on its ellipse. These figures also show that the falling limbs of the newer floods are approaching each other, while the falling limbs of the earlier floods form another group. The rotation angles are also visibly different. When analyzing the parameters of Tab for the first six sections, the average semi-major axis is typically smaller during smaller floods (as in December of 2023 and June of 2024), than during higher floods. The sections for ELTE-1 and GWM-21 show differences from the other sections, and both of them are close to the new northern building, so that the flow regime to these two wells was obstructed. The sections of the two riverside wells (ELTE-2 and ELTE-3) show the largest specific discharges and also the greatest rotation angles and semiminor axis values during each flood, according to Tab. 1.

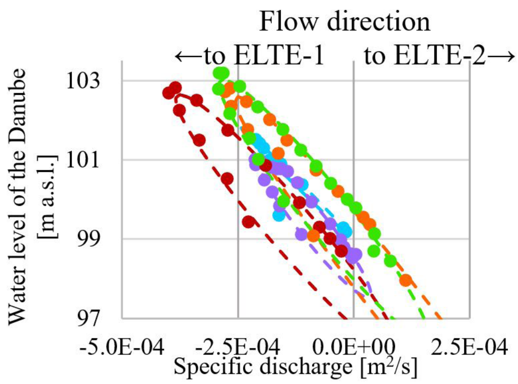

Fig. 16/a *ELTE-1 and ELTE-2*

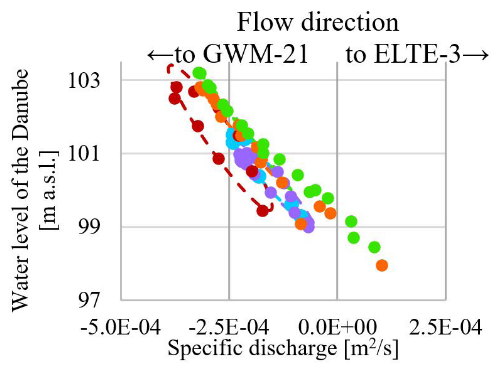

Fig. 16/ b *GWM-21 and ELTE-3*

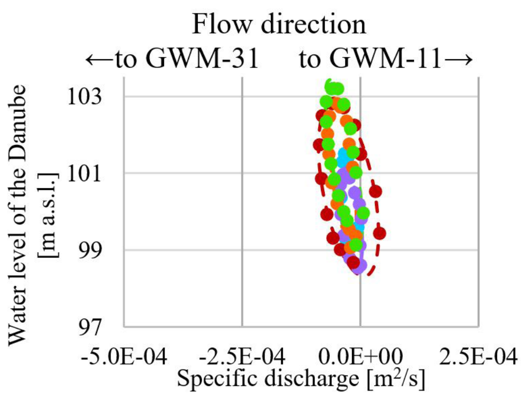

Legend for Fig. 16:
Flood in June, 2010
Flood in June, 2013
Flood in December, 2023
Flood in June, 2024
Flood in September, 2024

Fig. 16/c *GWM-31 and GWM-11*

Fig. 16 *Speci ic discharge in the sections between two wells perpendicular to the Danube*

More differences can be seen on the ellipses between the wells (as seen in Fig. 16). In the perpendicular sections (shown in purple in Fig. 2), the ratio of the semi-major axis and semi-minor axis changes, which thereupon changes the shape of the ellipses. For example, for the GWM-21 – ELTE-3 sections, the difference between the rising and falling limbs was much smaller before the new buildings than they are today. The rotation angle of GWM-31 and GWM-11 is the smallest of these three sections, as seen in Tab. 1, and this section also has the smallest specific discharge values.

An investigation of the parallel sections (blue lines in Fig. 2) is shown in Fig. 17. They indicate that the flow could reach the area behind the buildings more directly before, but the newer ellipses show smaller specific discharge values and even change in the direction of the flow. This is most visible in sections GWM-31 - GWM-21 (Fig. 17/a) and GWM-11 – ELTE-1 (Fig.17/c), and also in Tab. 1.

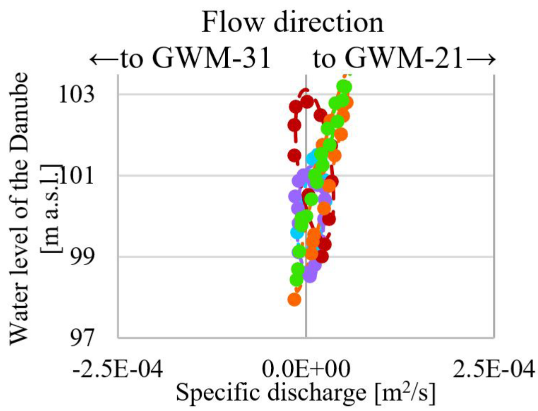

Fig. 17/ a *GWM-31 and GWM-21*

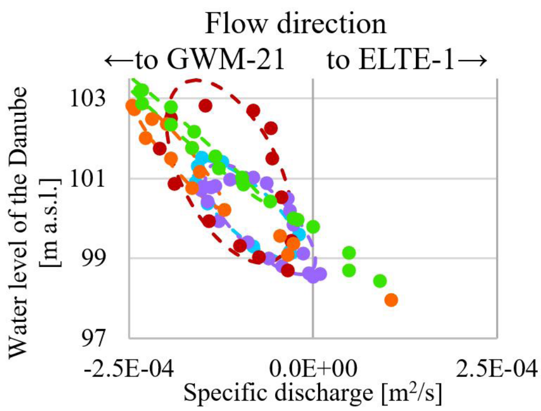

Fig. 17/ b *GWM-21 and ELTE-1*

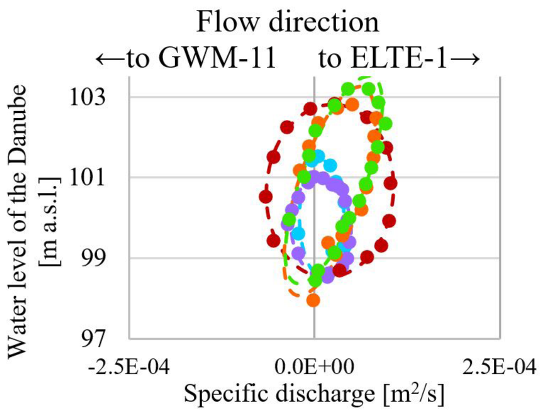

Fig. 17/ c *GWM-11 and ELTE-1*

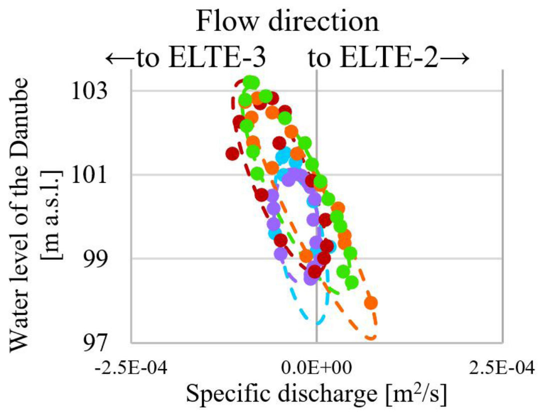

Fig. 17/ d *ELTE-3 and ELTE-2*

Fig. 17 *Specific discharges in the sections between two wells, parallel to the Danube, and presented with the water level of the Danube (Infopark)*

Legend for Fig. 17:
Flood in June, 2010; Flood in June, 2013; Flood in December, 2023
Flood in June, 2024; Flood in September, 2024

5.1 Comparison to another area

To further investigate the anthropogenic and natural effects on the loop curves and their ellipses, three riverside groundwater wells were examined for the same calculations. They are outside any urban areas, without any major interventions, and have data series for all the five floods examined. The first is Well 132141 near Apostag, and it is roughly 300 m away from the Danube. The second one is the Well 1455 near Uszód, which is 800 m away from the Danube. The third one, i.e., Well 132200, is near Sükösd, and is roughly 300 m away from the river. Their data series and the water level of the Danube were also available online on the website of the General Directorate of Water Management. The water level of the river was also interpolated between the daily averages of two neighbouring gauges. The geological data were estimated from the works of Mike (1991), and the aquifer typically has a high degree of conductivity, as it is formed of sediment deposited by the Danube. The main characteristics of the sections are presented in Tab. 2.

Vol. 33, 2025, No. 4, 54– 66

Tab. 2 *Main characteristics of the sections in the rural area*

Name of the well	Neighbouring gauges	Hydraulic conductivity [m/s]	Length of the section [m]	Level of the base [m a.s.l.]
132141 Apostag (1566.1 rkm)	Dunaújváros (1580.6 rkm) Dunaföldvár (1560.6 rkm)	$6.9{\cdot}10^{-3}$	~ 345	~ 83
1455 Uszód (1523.4 rkm)	Paks (1531.3 rkm) Dombori (1506.8 rkm)	$1.5{\cdot}10^{-2}$	~ 820	~ 80
132200 Sükösd (1494.2 rkm)	Dombori (1506.8 rkm) Baja (1478.7 rkm)	$6.9{\cdot}10^{-3}$	~ 245	~ 75

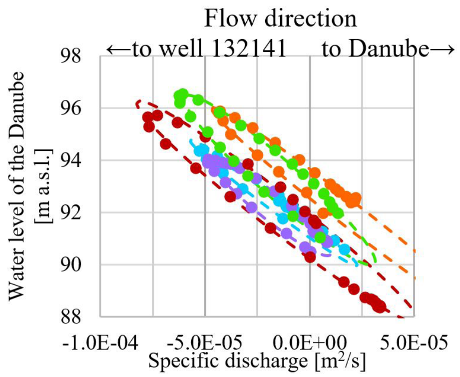

Fig. 18 *Specific discharge on the section between well 132141 and the Danube, presented with the water level of the Danube (Apostag)*

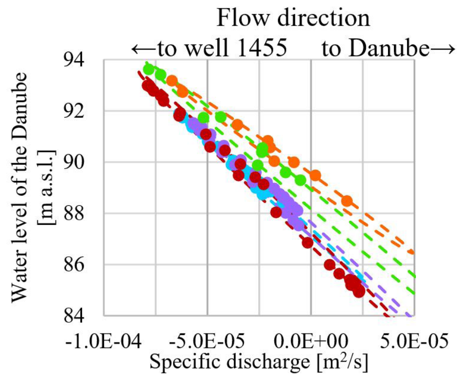

Fig. 19 *Specific discharge on the section between well 1455 and the Danube, presented with the water level of the Danube (Uszód)*

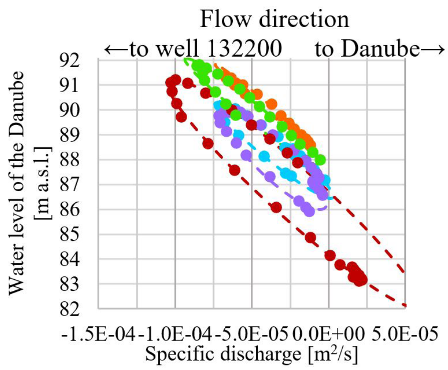

Fig. 20 *Specific discharge on the section between well 132200 and the Danube, presented with the water level of the Danube (Sükösd)*

Legend for Figs. 18-20.:
- Flood in June, 2010
- Flood in June, 2013
- Flood in December, 2023
- Flood in June, 2024
- Flood in September, 2024

A well-marked shift between the earlier and newer ellipses is also shown in Figs. 18-20, which indicates that the nature of the specific groundwater discharge can change due to natural effects and not only those caused by constructions and buildings. The rotation angles do not vary to the same extent, like they did in the INFOPARK study area. The sections in Figs. 18-20 are in the same range of lengths as the sections in INFOPARK, and they show the previously experienced hyteresis. The section near Uszód (Fig. 19) is much longer, and the shape of the curves differ. In Wagner, 2023 it was determined that the hysteresis did not occur in 3 km and 10 km long sections and that their approximation should be done linearly. In the section near Uszód, the difference between the rising limb still shows, as opposed to 2010 and 2013, when the initial groundwater table was higher.

By comparing the ellipses of the urban and rural sections, the natural effects can be viewed. The total change in the form of the ellipse, the ratio of the semi-major and semi-minor axes, and the drastic change in the rotation angle are all caused by anthropogenic interventions, as they are missing in the rural sections. However, the shift in the ellipses occurs in both types of sections, which is caused by the greater specific discharge values. As shown in Figs. 11-14, the greater the difference between the water level of a well and a river results in a larger slope, which also means greater specific discharge values. This goes to show that the shift of the ellipses is in relation to the difference in the initial water level, which was in relation to the initially lower groundwater table after the recent droughts. Also, a small change in the ratio is also detected at the rural section near Uszód, so natural causes also affect this relation to a lesser extent in some cases.

5.2 Analysis of the ellipse parameters

Quantifying the changes in the parameters of each ellipse was the next step to further analyze the connections. These parameters were a product of the process of creating the ellipses. First, the rotation angles were examined, which were given in radians; $\pi/2$ was subtracted from each angle, for a better presentation of the changes in the direction of the main flow. Their deviation from $\pi/2$ is presented in Fig. 21. The greater rotation angle means a greater specific discharge in each section, if the other parameters are the same. In the sections GWM-21 – GWM-31 and ELTE-1 – GWM-11, the rotations drastically change. The ellipse points to the other end of the section, which indicates that the newest buildings obstruct the groundwater regime and that the direction of the flow is in the direction opposite than before. The river cannot seep through this area as easily as it did when the buildings were not there.

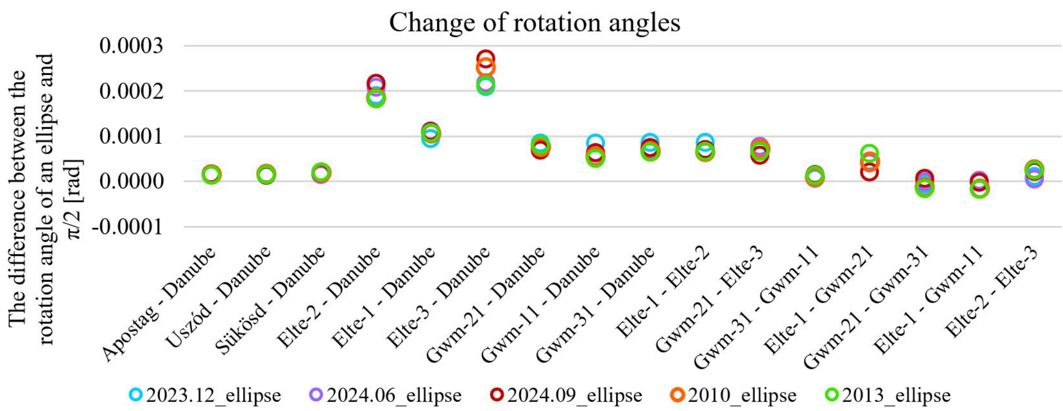

Fig. 21 *Change of rotation angles*

As a greater slope of a section could similarly mean a larger specific discharge, the linear correlation between the greatest slope at every flood and rotation angle was examined. As the data series are not homogeneous, the correlation should be considered with care and mainly used to search for anomalies. The relationship is strong when it is close to 1, and there is no connection when it is 0. In the case of a linear regression, the factor is determined according to Eq. 5 (Kontur et al., 1993). To have a better understanding of its reliability, the root-mean-square error (RMSE) is used, which can be computed with Eq. 6 (Hodson, 2022).

$$Correlation\ factor = \frac{\sum_{i=1}^{N} \Delta x_i \cdot \Delta y_i}{N \cdot \sigma_x \cdot \sigma_y} \quad (5)$$

where x is the rotation angle; y is the greatest slope of a section at each flood; σ is the standard deviation of a variable; and N is the amount of data used.

$$RMSE = \sqrt{\frac{\sum_{i=1}^{N} (\hat{x}_i - x_i)^2}{N}} \quad (6)$$

where x is the rotation angle [rad]; and N is the amount of data used.

The correlation factors are shown in Tab. 3. The negative correlation factor (dark orange) shows that if all the other parameters were the same, the flood would be more significant in a westerly (perpendicular) or southerly (parallel section) direction than it was before the constructions and that the specific discharge would be greater in this direction. The positive correlation factor (pale orange) shows that the same flood had lost its effect in these sections and that the specific groundwater discharges would be smaller than before. The higher RMSE values (coloured in red) show the sections with the greatest changes after the new buildings were constructed.

Tab. 3 *Correlation of the slope and rotation angle of an ellipse*

Correlation between the slopes and rotation angles	Apostag – Danube	Uszód - Danube	Sükösd - Danube	Elte-2 - Danube	Elte-1 - Danube	Elte-3 - Danube	Gwm-21 - Danube	Gwm-11 - Danube	Gwm-31 - Danube	Elte-1 - Elte-2	Gwm-21 - Elte-3	Gwm-31 - Gwm-11	Elte-1 - Gwm-21	Gwm-21 - Gwm-31	Elte-1 - Gwm-11	Elte-2 - Elte-3
Correlation factor	-0.0020	0.56	0.27	-0.37	-0.36	-0.66	0.15	0.16	0.09	0.19	0.63	-0.68	-0.16	-0.43	-0.24	-0.68
RMSE	1.1E-06	1.1E-06	1.8E-06	1.2E-05	5.4E-06	1.4E-05	5.8E-06	1.1E-05	7.9E-06	7.6E-06	4.2E-06	1.5E-06	1.3E-05	6.9E-06	8.2E-06	4.6E-06

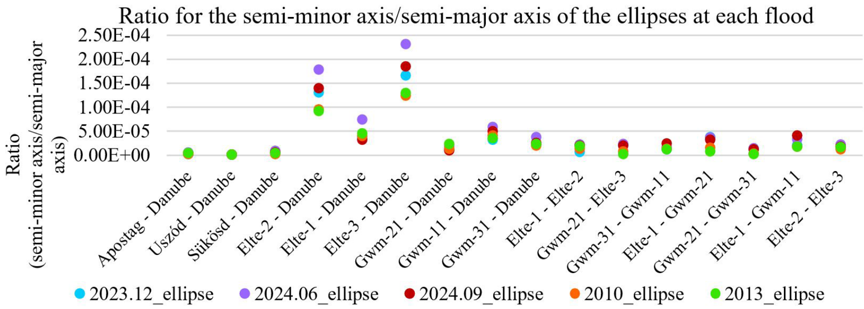

Fig. 22 *Ratio of the ellipses (semi-minor axis/semi-major axis)*

Next, the ratio between the semi-minor axis and semi-major axis was investigated in each section, as seen in Fig. 22. These calculations are specific to the currently used dimensions (m a.s.l. for the water level and m^2/s for the specific discharge). The larger ratio means a more rounded ellipse, with a greater difference in the rising and falling limbs. The more elongated ellipses with smaller ratios do not show such differences between the limbs of the flood.

The relationship between the two axes was computed with a linear correlation factor (Eq. 7). The greater RMSE value shows the sections with the more significantly different ellipses (Eq. 8) and are shown in Tab. 4. As the magnitude of the semi-minor axis differs in each section, the percent bias (PBIAS) was computed for the two floods with Eq. 9 (Gupta et al., 1999). If the PBIAS is negative (blue cells), the ratio is bigger in the calculated data than the linear correlation equation suggests, which means that an ellipse is rounder and that the difference of the falling and rising limbs is actually greater. The positive PBIAS (orange cells) means the predicted ratio belongs to a more rounded ellipse than the actual ellipse from the data calculated, which is more elongated. The difference between the rising and falling limbs is smaller.

$$Correlation\ factor = \frac{\sum_{i=1}^{N} \Delta z_i \cdot \Delta w_i}{N \cdot \sigma_x \cdot \sigma_y} \tag{7}$$

where z is the semi-major axis [m]; w is the semi-minor axis [m^2/s]; σ is the standard deviation of a variable; and N is the amount of data used.

$$RMSE = \sqrt{\frac{\sum_{i=1}^{N} (\hat{w}_i - w_i)^2}{N}} \tag{8}$$

where w is the semi-minor axis [m^2/s], and N is the amount of data used.

$$PBIAS = \frac{\sum_{i=1}^{N} (\hat{w}_i - w_i) \cdot 100}{\sum_{i=1}^{N} w_i} \tag{9}$$

where w is the semi-minor axis [m^2/s], and N is the amount of data used.

Tab. 4 *Correlations between the semi-major axis and semi-minor axis*

Correlation between semi-major axis and semi-minor axis of the ellipses	Apostag - Danube	Uszód - Danube	Sükösd - Danube	Elte-2 - Danube	Elte-1 - Danube	Elte-3 - Danube	Gwm-21 - Danube	Gwm-11 - Danube	Gwm-31 - Danube	Elte-1 - Elte-2	Gwm-21 - Elte-3	Gwm-31 - Gwm-11	Elte-1 - Gwm-21	Gwm-21 - Gwm-31	Elte-1 - Gwm-11	Elte-2 - Elte-3
Correlation factor	0.45	0.56	-0.19	0.28	0.67	0.38	0.61	0.63	0.63	0.66	0.18	0.59	0.34	-0.45	0.27	0.40
RMSE	4.4E-06	1.2E-06	4.4E-06	1.1E-04	9.1E-06	9.5E-05	1.5E-05	2.0E-05	1.1E-05	1.6E-05	5.5E-05	1.3E-05	4.5E-05	9.3E-06	5.3E-05	8.0E-06
PBIAS for 2024.09. [%]	20.49	40.18	22.47	0.02	1.09	-11.28	34.21	-6.99	-3.30	-17.94	181.16	-9.57	76.57	-35.48	-25.79	-10.22
PBIAS for 2010 [%]	63.89	-45.66	73.67	50.08	6.64	36.21	2.44	7.32	23.81	39.78	-111.38	43.58	-76.32	-151.71	135.09	43.09

The PBIAS was examined on the flood data in 2010 and in September 2024, which were two floods similar in height. These results show the deviation of the semi-minor axis calculated from the value modelled. The PBIAS was used to reveal the sections, the ellipses of which differed the most from each other during the two floods. More daily data series in a section during floods used in the linear correlation would result in a clearer comparison.

6 CONCLUSIONS

In this work, the effect of two new riverside buildings were examined with the help of several sections located in different directions to describe any change in the natural relationship between the groundwater and river due to the constructions. In this process, the effects of recent droughts also were noted. Calculations were also done for wells in rural areas for purposes of comparison. The figures of the specific discharges with the water level of the river created loop curves that are approachable with ellipses. The parameters of these ellipses describe and quantify the changes in the loop curves and gives an opportunity to characterize them further.

The two new riverside buildings obstructed the groundwater regime in the area, which resulted in different specific discharge values. They show that previously, the flow had reached the area behind the buildings more directly, but the newer ellipses show smaller specific discharge values and even changes in the direction of the flow.

Such an investigation may help to understand the processes in the municipal underground environment in the case of riverine floods. It could lead to an explanation of, and possibly the solution to, problems that arise near buildings of several storeys below ground level that cross an aquifer. Further investigation of the anthropogenic and natural changes in the groundwater-surface water relationship could help modellers when studying bank storage or examining and estimating the components of the water balance of a site. These insights are valuable for designing drainage systems, reinforcing foundations, and guiding urban planning decisions to mitigate flood-related impacts.

REFERENCES

CSOMA, Rózsa; GÁLOS, Miklós. *River–groundwater interaction over the region of Infopark-Budapest,* Periodica Polytechnica (2012) Vol. 56/2, Available at https://doi.org/10.3311/pp.ci.2012-2.08

DARCY, Henry. *Les Fontaines Publiques de la Ville de Dijon* (1856) Paris. 647 pp.

General Directorate of Water Management (https://data.vizugy.hu/).

GODLEWSKI, Tomasz; BOGUSZ, Witold; KACZYŃSKI, Łukasz. C*hange in groundwater conditions as a cause of structural failure - selected case studies.* MATEC Web of Conferences, vol. 284 (2019) 03001, Available at: https://doi.org/10.1051/matecconf/201928403001

GUPTA, Hoshin; SOROOSHIAN, Soroosh; YAPO, Patrice. *Status of Automatic Calibration for Hydrologic Models: Comparison With Multilevel Expert Calibration.* Journal of Hydrologic Engineering, vol. 4 (1999), No. 2, Available at: https://doi.org/10.1061/(ASCE)1084-0699(1999)4:2(135)

HENDEL, Tal. Ellipse Fit, MATLAB Central File Exchange (2008) Availablet at: https://www.mathworks.com/matlabcentral/fileexchange/22423-ellipse-fit [retrieved 2025-05-01]

HODSON, Timothy. O. *Root-mean-square error (RMSE) or mean absolute error (MAE): when to use them or not,* Geosci. Model Dev. vol. 15 (2022), pp. 5481–5487, Available at: https://doi.org/10.5194/gmd-15-5481-2022

HORUSITZKY, Henrik. B*udapest Székesfőváros hidrogeológiai viszonyai (Hydrogeological conditions of the capital city of Budapest)* Hidrológiai Közlöny, Vol. XII. (1932) No. 1.

IHRIG, Dénes. (1973) *A magyar vízszabályozás története (The history of Hungarian water regulations),* VIZDOK, Budapest, Hungary

KALBUS, Edda; REINSTORF, Frido; SCHIRMER, Mario. *Measuring methods for groundwater - surface water interactions: a review.* Hydrology and Earth System Sciences, vol. 10 (2006). No. 6, pp. 873-887. Available at: https://doi.org/10.5194/hess-10-873-2006

KUKUCSKA, Péter; GÁLOS, Miklós; CSOMA, Rózsa. (2015). *Tározódás talajban dunai árhullámok esetén (Storage in the ground in case of flood waves on the Danube)* Mérnökgeológia-Kőzetmechanika, Hantken Kiadó, pp. 25-40, Budapest

MIKE, Károly. (1991), *Magyarország ősvízrajza és felszíni vizeinek története* (The prehistoric hydrography and history of Hungary's surface waters) AQUA Kiadó, Budapest

NAGY, Tamás A 2013. júniusi és a 2024. *szeptemberi dunai árhullám értékelése a folyami vízállások, a háttérre vonatkozó talajvízszint eloszlások, valamint a kialakult árvízi jelenségek összefüggéseinek tükrében (Evaluation of the Danube flood waves of June 2013 and September 2024 in light of the relationships between river water levels, background groundwater level distributions, and the flood phenomena that occurred)* Hungarian Hydrological Society, (2025) Available at: https://www.hidrologia.hu/vandorgyules/42/word/0114_nagy_tamas.pdf

SZIVÓS, Balázs; CSOMA, Rózsa; GÁLOS, Miklós. (2013), *A Darcy-féle áteresztőképességi együttható eloszlásának vizsgálata a Lágymányosi-öblözet területén* (Investigation of the distribution of the Darcy hydraulic conductivity in the region of Lágymányos) Mérnökgeológia – Kőzetmechanika, Hantken Kiadó, pp.19-28, Budapest

WAGNER, Flóra. (2018) *A lágymányosi mintaterület talajvíz-hidraulikai modellje (The groundwater model of the Lágymányos pilot area),* BSc Diploma thesis, Budapest University of Technology and Economics

WAGNER, Flóra. *The effect of underground structures on the groundwater flow introduced at a riverside pilot area in Budapest International Conference of Young Scientists on Energy and Natural Sciences Issues* (CYSENI), vol. 18 (2022), pp. 771–782

WAGNER, Flóra; CSOMA, Rózsa. *A felszín alatti áramlás vizsgálata árvíz idején (Investigation of groundwater flow during floods),* Hungarian Hydrological Society, (2025) Available at: https://www.hidrologia.hu/vandorgyules/40/word/0226_wagner_flora.pdf

WINTER, Thomas C.; HARVEY, Judson W.; FRANKE, O. Lehn; ALLEY, William M. (1998). *Ground Water and Surface Water: A Single Resource.* U.S. Geological Survey Circular 1139, 79 pp. Available at: https://pubs.usgs.gov/circ/circ1139/